Energy Proceedings
Vol 59, 2025
ISSN 2004-2965

Toward A Novel Energy Internet Paradigm: Distributed Cooperative Control of Heterogeneous DREs in Hybrid AC/DC Microgrids#

Xing Huang[1], Yulin Chen[2*], Donglian Qi[1,2*], Ying Weng[3] , Yucan Zhang[1], Guangxin Zhi[2]

1 College of Electrical Engineering, Zhejiang University, Hangzhou 310012, China

2 Hainan Institute of Zhejiang University, Sanya 572024, China

3 Polytechnic Institute, Zhejiang University, Hangzhou 310015, China
(Yulin Chen: chenyl2017@zju.edu.cn and Donglian Qi: qidl@zju.edu.cn)

ABSTRACT

To facilitate the integration of heterogeneous distributed renewable energy sources (DREs), hybrid AC/DC microgrids (MGs) are constructed by synthesizing the inherent advantages of AC and DC MGs, emerging as promising grid architectures. Among them, the interlinking converter (ILC) serves as the critical interface connecting AC and DC subgrids while enabling bidirectional power exchange. Considering the system deviations caused by droop control and the additional complexity introduced by ILC integration, a distributed cooperative control strategy in hybrid AC/DC MGs is proposed in this paper for coordinating heterogeneous DREs and ILCs within the energy internet paradigm. A comprehensive hierarchical cooperative control framework is established, within which the proposed strategy achieves simultaneous frequency and voltage restoration, proportional power/current sharing and regulated inter-subgrid power exchange. Theoretical stability analysis and detailed simulation studies demonstrate the efficacy of the proposed control strategy.

Keywords: Energy internet paradigm, distributed cooperative control, heterogeneous DREs, interlinking converter, hybrid AC/DC microgrids

1. INTRODUCTION

To tackle the grid operational challenges induced by high-penetration distributed renewable energy sources (DREs), the Energy Internet has emerged as a transformative paradigm, enabling bidirectional cyber-physical integration of power and information flows [1]. The inherent multi-domain coupling nature of the Energy Internet introduces new challenges and opportunities, driving considerable cross-disciplinary research [2]. Typically, the critical components and techniques utilized in the Energy Internet are divided into power systems, communication networks, and control algorithms. Within this framework, microgrids (MGs) serve as fundamental parts of the Energy Internet, facilitating renewable penetration, enabling localized energy management, and optimizing overall system performance [3].

MGs are typically summarized into two categories according to the bus configuration and sources/loads characteristics [4], namely, AC MGs [5] and DC MGs [6]. Notice that, DREs mainly exhibit native DC output characteristics. Consequently, AC MGs suffer from compromised power conversion efficiency and elevated capital expenditures when integrating DC-coupled DREs. Furthermore, the rapidly increasing penetration of DC loads necessitates additional AC/DC conversion stages in conventional AC MGs, further degrading system-wide efficiency [7]. Given the entrenched predominance of AC infrastructure, exclusive DC network development remains impractical. Simultaneously, substantial existing AC loads mandate a hybrid approach. Therefore, hybrid AC/DC MGs have emerged as a critical solution [8], [9].

Recently, many researchers have paid attention to studying the hybrid AC/DC MGs [10]. However, existing research methods predominantly focus on centralized and decentralized control strategies [11], [12], with particular emphasis on the economic-low-carbon operation and energy optimization management of the hybrid MGs. For instance, [12] designed a decentralized MPC control strategy to maximize power utilization and enhance system performance. Moreover, the bidirectional interlinking converters (ILCs) are well designed to bridge AC and DC MGs, eliminating redundant conversion consumption and providing native interfaces for both DC and AC devices [13]. Despite the

This is a paper for the 11th Applied Energy Symposium: Low Carbon Cities & Urban Energy Systems (CUE2025), July 18-22, 2024, Kitakyushu, Japan.

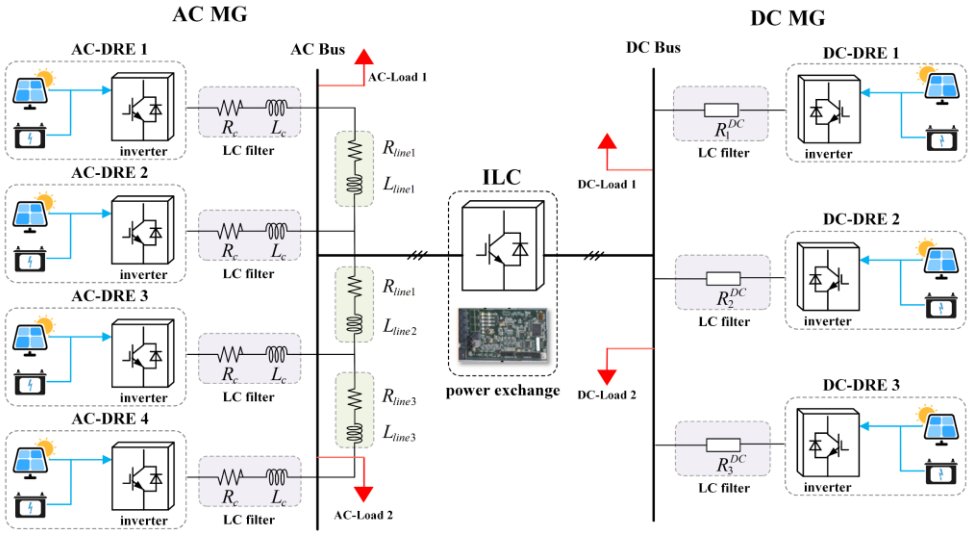

Fig. 1 Diagram of the test hybrid AC/DC MG, including the AC MG, DC MG and ILC.

critical role of as key components for grid interconnection, rare studies have investigated frameworks and strategies for ILC participation in the distributed coordinated operation of the hybrid AC/DC MGs.

To solve theses problems, we propose a distributed coordination control strategy for hybrid AC/DC MGs to ensure simultaneous fair power/current sharing, accurate voltage/frequency restoration, and real-time inter-subgrid power exchange.

2. HYBRID AC/DC MICROGRID CONFIGURATION

2.1 Graph Theory

Consider a hybrid AC/DC MG system containing M DREs, with $n^*(n^* < M)$ DREs located in AC MG and the remaining $m^*(m^* = M - n^*)$ DREs situated in DC MGs. The associated communication network is characterized by graph $\mathcal{G}_M = (\mathcal{V}_M, \mathcal{E}_M)$. $\mathcal{V}_M$ and $\mathcal{G}_M = (\mathcal{V}_M, \mathcal{E}_M)$ refer to the node and edge set, respectively. $\mathcal{N}_i$ is defined as the set of the neighbors of DRE i. Denote the adjacent matrix as $\mathcal{A}_M = [a_{ij}]_{M\times M}$, where $a_{ij} \in 0,1$ and $a_{ij} = 1$ means that DRE i can receive the information from DRE j. The Laplacian matrix of graph $\mathcal{G}_M$ is represented as $\mathcal{L}_M = [l_{ij}]_{M\times M}$, i.e.,

$$l_{i,j} = \begin{cases} -a_{ij} & i \neq j \\ \sum_{j\in N_i^M} a_{ij} & \text{otherwise} \end{cases}. \tag{1}$$

2.2 Droop-based Primary Control

In an AC MG, the droop control is mainly adopted to autonomously accomplish proportion power sharing according to DRE's capacity while maintaining system frequency/voltage stability and ensuring supply/demand balance. Specifically,

$$\begin{aligned} \omega_i(t) &= \omega_i^{nom} - K_i^p \cdot P_i^{AC}(t), \\ E_i(t) &= E_i^{nom} - K_i^q \cdot Q_i^{AC}(t), \end{aligned} \tag{2}$$

where $\omega_i(t)$ and $E_i(t)$ are the output frequency and voltage of DRE i. ω_i^{nom} and E_i^{nom} are the corresponding nominal values. K_i^p and K_i^q are the droop coefficients. $P_i^{AC}(t)$ and $Q_i^{AC}(t)$ are the output active and reactive power.

Similarly, droop-based primary control in a DC MG aims at achieving current sharing and voltage restoration. Thus, the voltage reference $V_i^{ref}(t)$ can be modeled as follows

$$V_i^{ref}(t) = V_{nom} - d_i^{DC} \cdot I_i^{DC}(t), \tag{3}$$

where V_{nom} is the pre-designed nominal DC voltage value. $I_i^{DC}(t)$ is the current of DRE i.

Fig. 1 depicts the diagram of the test DC MG. If the transmission line R_i^{DC} is taken into consideration, the bus voltage $V_b(t)$ is calculated as

$$V_b(t) = V_i^{ref}(t) - R_i^{DC} \cdot I_i^{DC}(t). \tag{4}$$

Combing equation (3) and (4), we have

$$V_b(t) = V_{nom} - (R_i^{DC} + d_i^{DC}) \cdot I_i^{DC}(t). \tag{5}$$

Due to $d_i^{DC} \gg R_i^{DC}$ holds, the current sharing ratio

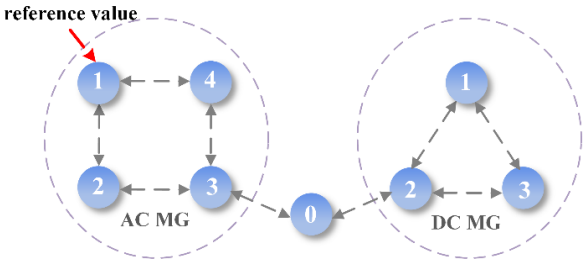

Fig. 2 Communication structure of the test hybrid AC/DC MG

is dictated by the fixed droop coefficient d_i^{DC}. Therefore, the output current satisfies

$$\frac{I_i^{DC}(t)}{I_j^{DC}(t)} = \frac{R_j^{DC} + d_j^{DC}}{R_i^{DC} + d_i^{DC}} \approx \frac{d_j^{DC}}{d_i^{DC}}. \tag{6}$$

From equation (5), we can find that when $I_i^{DC}(t) \neq 0$, $V_b(t) \neq V_{nom}$ holds.

Since frequency in AC subgrids and DC bus voltage in DC subgrids represent distinct droop parameters, normalizing $\omega_i(t)$ and $V_b(t)$ to per-unit quantities $\omega_i^{p.u}(t)$ and $V_b^{p.u}(t)$ is necessary, using the following equation

$$\begin{aligned} \omega_i^{p.u}(t) &= \frac{\omega_i(t) - 0.5(\omega_{max} + \omega_{min})}{0.5(\omega_{max} - \omega_{min})}, \\ V_b^{p.u}(t) &= \frac{V_b(t) - 0.5(V_{max} + V_{min})}{0.5(V_{max} - V_{min})}, \end{aligned} \tag{7}$$

where ω_{max}, ω_{min}, V_{max} and V_{min} refer to the maximum and minimum frequencies in AC subgrids, voltages in DC subgrids, respectively.

2.3 Secondary Control Objectives

1) Restore the frequencies of DREs in AC subgrids to the rated values, represented as

$$\lim_{t\to\infty} \omega_i(t) = \omega_{rated}, \tag{8}$$

where ω_{rated} is the reference value.

2) Maintain the DC bus voltage at the nominal setpoint, represented as

$$\lim_{t\to\infty} V_b(t) = V_{nom}, \tag{9}$$

where V_{nom} is the pre-designed nominal voltage value.

3) Active power sharing among all DREs is allocated by proportional dispatch principle based on their maximum capacities, represented as

$$\lim_{t\to\infty} \frac{P_i(t)}{P_i^{max}} = \frac{P_j(t)}{P_j^{max}}, \tag{10}$$

where P_i^{max} and P_j^{max} refer to the maximum capacity of the DRE i and DRE j.

4) The current sharing ratios of DREs are inversely proportional to their droop coefficients, represented as

$$\frac{I_i^{DC}(t)}{I_j^{DC}(t)} = \frac{d_j^{DC}}{d_i^{DC}}, \tag{11}$$

5) The ILC aims to stabilize hybrid AC/DC MGs by regulating bidirectional power flow between subgrids, represented as

$$\lim_{t\to\infty} P_0^{ILC}(t) = \lim_{t\to\infty} P_{sum}^{AC}(t) - \sum_{i=1}^{m} P_i^{AC}(t), \tag{12}$$

where $P_{sum}^{AC}(t)$ is the total load. $P_0^{ILC}(t)$ is ILC's power.

3. DISTRIBUTED COOPERATIVE CONTROL STRATEGY OF HETEROGENEOUS DRES

To compensate for the frequency deviations in the AC subgrids and voltage deviations in the DC subgrids, we design a consensus-based distributed cooperative control strategy.

For the AC MG, differentiating equation (2b), we have

$$\dot{\omega}_i(t) = \dot{\omega}_i^{nom} - K_i^p \cdot \dot{P}_i^{AC}(t) = u_{\omega,i}^{AC}(t), \tag{13}$$

where $u_{\omega,i}^{AC}$ is the auxiliary frequency variable.

With the application of the consensus-based algorithm, $u_{\omega,i}^{AC}(t)$ can be formulated as

$$u_{\omega,i}^{AC}(t) = -\beta_{\omega,i} \sum_{j\in\mathcal{N}_i} a_{ij}\left(\omega_i(t) - \omega_j(t)\right) - \beta_{\omega,i} \cdot g_i\left(\omega_i(t) - \omega_{rated}\right) \tag{14}$$

where $\beta_{\omega,i}$ is the frequency control gain. Connection gain $g_i = 1$ means that DRE \$i\$ can receive the reference value.

Recalling equation (13), ω_i^{nom} can be derived as

$$\omega_i^{nom} = \int \left(u_{\omega,i}^{AC}(t) + K_i^p \cdot \dot{P}_i^{AC}(t)\right) dt. \tag{15}$$

At the same time, the output active power of each DRE needs to be regulated in proportional to the capacities. Therefore, the auxiliary power variable $u_{p,i}^{AC}(t)$ is designed according to the following equation

$$u_{p,i}^{AC}(t) = -\beta_{p,i} \sum_{j \in \mathcal{N}_i} a_{ij} \left(K_i^p \cdot P_i^{AC}(t) - K_j^p \cdot P_j^{AC}(t) \right), \quad (16)$$

where $\beta_{p,i}$ is the power control gain.

Consequently, equation (15) can be rewritten as

$$\omega_i^{nom} = \int \left(u_{\omega,i}^{AC}(t) + u_{p,i}^{AC}(t) \right) dt. \quad (17)$$

Tab.1 Parameters of the test AC MG

	DRE 1&DRE 2		DRE 3&DRE 4	
DREs	$R_{c1,2}$	0.2	$R_{c3,4}$	0.2
	$L_{c1,2}$	3×10^{-3}	$L_{c3,4}$	3×10^{-3}
	$P_{1,2}^{max}$	10640	$P_{3,4}^{max}$	8000
	$K_{1,2}^p$	9.85	$K_{3,4}^p$	7.4
	Line 1 & Line 3		Line 2	
Lines	$R_{\text{line1,3}}$	0.23	R_{line2}	0.35
	$L_{\text{line1,3}}$	0.318×10^{-3}	L_{line2}	1.847×10^{-3}
	Load 1		Load 2	
Loads	P_{L1}^{AC}	7×10^{3}	P_{L2}^{AC}	15.6×10^{3}

Tab.2 Parameters of the test DC MG

	DRE1		DRE2		DRE3	
DREs	V_{DC}	200	V_{DC}	200	V_{DC}	200
	f_s	20 k	f_s	20 k	f_s	20 k
	d_1^{DC}	8	d_2^{DC}	4	d_3^{DC}	2
	Line 1		Line 2		Line 3	
Lines	R_1^{DC}	0.1	R_2^{DC}	0.1	R_3^{DC}	0.1
	Load 1		Load 2			
Loads	R_{L1}^{DC}	50	R_{L2}^{DC}	40		

Similarly, for the DC MG, we adopt the distributed cooperative control strategy to realize the bus voltage restoration. Based on equation (5), the distributed secondary voltage control variable $u_{v,i}^{DC}$ is then introduced to precisely recover the bus voltage to the nominal setpoint, i.e.,

$$V_b(t) = V_{nom}(t) - (R_i^{DC} + d_i^{DC}) \cdot I_i^{DC}(t) + u_{v,i}^{DC}(t). \quad (18)$$

By applying the consensus algorithms, $u_{v,i}^{DC}$ is

$$u_{v,i}^{DC}(t) = \mathcal{H}_{P,i} \cdot e_{v,i}^{DC}(t) + \mathcal{H}_{I,i} \int e_{v,i}^{DC}(t) dt \quad (19)$$

where $\mathcal{H}_{P,i}$ and $\mathcal{H}_{I,i}$ are the proportional gain and the integral gain. $e_{v,i}^{DC}(t)$ is the consensus errors, defined as

$$e_{v,i}^{DC}(t) = -\alpha_{v,i} \sum_{j \in \mathcal{N}_i} a_{ij} \left(u_{v,i}^{DC}(t) - u_{v,j}^{DC}(t) \right) - \alpha_{v,i} \cdot g_i \left(V_b(t) - \omega_{rated} \right) \quad (20)$$

where $\alpha_{v,i}$ is the voltage control gain.

Therefore, frequency/voltage restoration and power/current sharing in subgrids can be realized after applying the distributed cooperative control strategy. Meanwhile, when the DC MG injects power into the AC MG, the ILC enables bidirectional energy exchange between AC and DC subgrids through power electronic conversion technologies.

4. CASE STUDIES

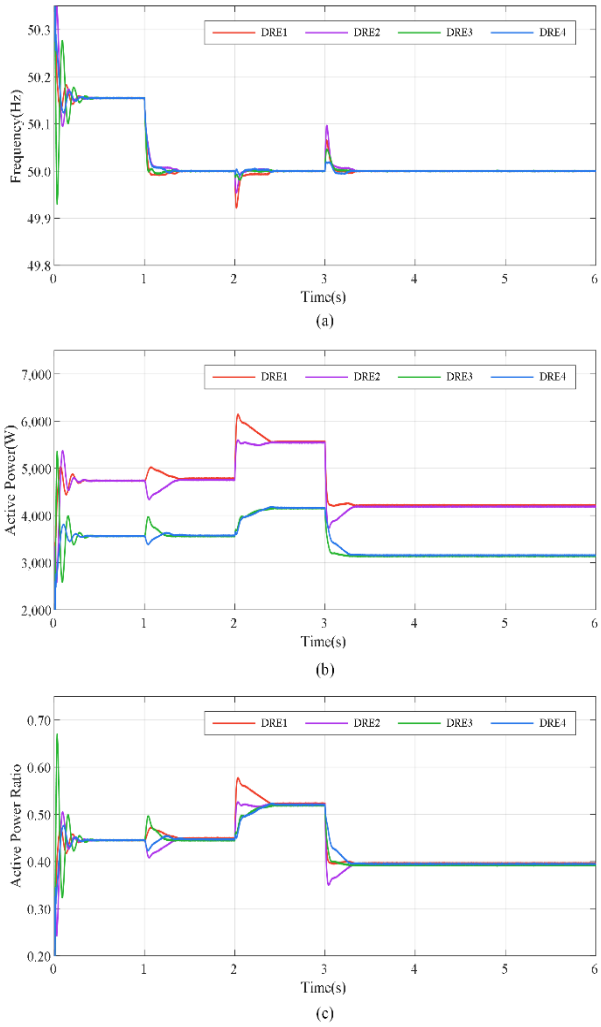

Fig. 3 Performance of the proposed strategy in the AC subgrid. (a) Frequency response. (b) Active power response. (c) Active power sharing ratio.

This section evaluates the distributed cooperative control strategy of heterogeneous DREs in hybrid AC/DC MGs under step load variations. The test hybrid AC/DC MG architecture and its communication network are illustrated in Fig. 1 and Fig. 2. Key parameters of the test subgrids are given in Table I and Table II. We define two metrics: the active power and current sharing ratios, i.e., $\psi_i^P = P_i(t) / P_i^{max}$ and $\psi_i^I = I_i^{DC}(t) / d_i^{DC}$. The simulation is conducted in the following stages.

1) During the initial 1 s, the AC MG operates only with droop-based primary control, while the DC MG employs the droop-based primary control exclusively until $t = 0.5$ s.

2) At $t=1$ s, the distributed cooperative control strategy is activated for DREs in the AC subgrid, whereas the DC subgrid utilizes the distributed cooperative control earlier at $t=0.5$ s.

3) At $t=2$ s, load 1 in the AC subgrid experiences a 3 kW step increase.

4) Subsequently, at $t=3$ s, the DC subgrid injects 5kW of active power into the AC subgrid via the ILC.

5) Finally, an additional resistive load $R_{L3}^{DC}=40\Omega$ is connected to the DC bus at $t=4$ s.

Fig. 3 presents the performance of the proposed strategy in the AC subgrid, depicting the frequency, active power, and active power ratio for each DRE. As seen from Fig. 3 (a), all DRE frequencies deviate from the reference value under primary control alone. However, after implementing the proposed strategy, the frequencies rapidly restore to 50 Hz. Combining Fig. 3 (b) and (c) shows that under load variation, the active power of all DREs can achieve fair sharing proportional to their capacities within a short time. When the DC MG injects 5kW of active power into the AC subgrid through the ILC at $t=3$ s, all DREs adjust their active power output proportionally in response to this power injection, thereby ensuring stable grid operation.

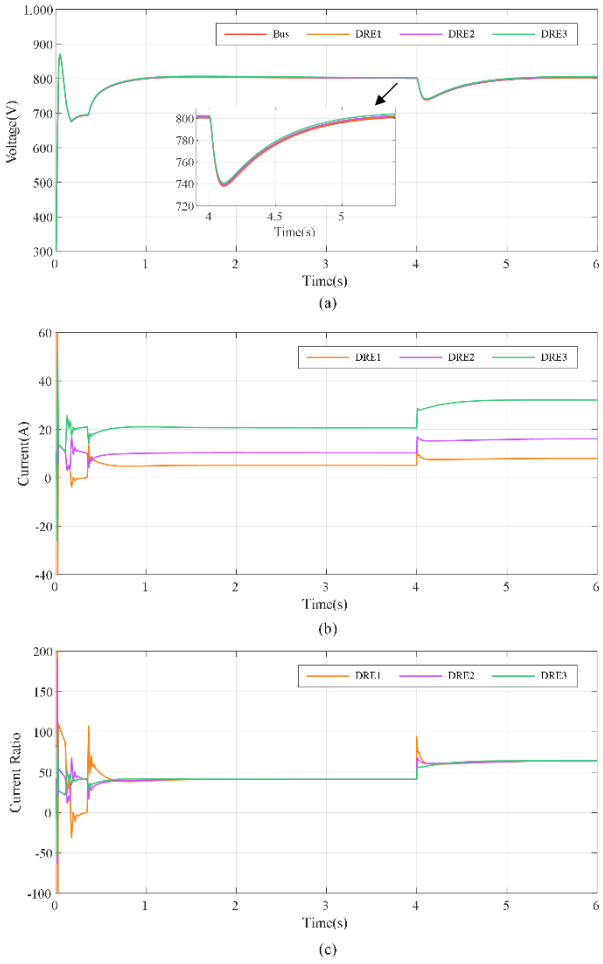

Fig. 4 Performance of the proposed strategy in the DC subgrid. (a) DC bus voltage and output voltage response. (b) Output current response. (c) Current sharing ratio.

The performance of the proposed strategy in the DC subgrid is illustrated in Fig. 4, including the DC bus voltage, output voltage, output current, and current-sharing ratio for each DRE. Fig. 4 (a) demonstrates that DC bus voltage V_b has a certain offset due to the droop-based primary control strategy, dropping below 700 V. However, it is observed that when the proposed distributed strategy is triggered at $t=0.5$ s, rapid voltage recovery to 800 V is realized, effectively compensating for voltage deviations induced by power transmission events launched at $t=3$ s and subsequent Load 3 integration at $t=4$ s. Furthermore, as depicted in Fig. 4 (b) and (c), the currents of all DREs increase proportionally and maintain the approximate rati $I_1^{DC}:I_2^{DC}:I_3^{DC}\approx d_3^{DC}:d_2^{DC}:d_1^{DC}=1:2:4$ throughout the simulation. The simulation results confirm that the proposed distributed cooperative control strategy regulates DC bus voltage while simultaneously maintaining current sharing property inherent to droop control, even during power exchange events and load variations.

The dynamic active and reactive power transmitted through the ILC is plotted in Fig. 5. As observed in Fig. 5,

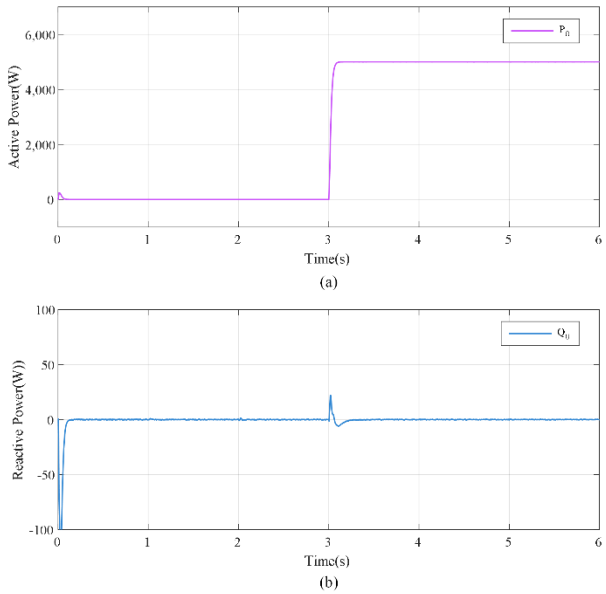

Fig. 5 Dynamic power exchange performance of the proposed strategy in the ILC. (a) Active power exchange through the ILC. (b) Reactive power exchange through the ILC.

the AC and DC subgrids on both sides of the ILC maintain power balance during the $t = 0 \sim 3$ s and $t = 3.15 \sim 6$ s intervals. Consequently, power transmitted through the ILC approaches zero, rendering them negligible. Critically, at $t = 3$ s, a 5kW active power injection event occurs. This disturbance is instantaneously reflected in the ILC power flow metrics, manifesting as 5kW active power transmission while reactive power remains unchanged. Subsequently, all DREs participate in coordinated power redistribution to guarantee the supply/demand equilibrium in the hybrid system. This simulation validates the ILC's indispensability role as the inter-subgrid energy exchange component.

5. CONCLUSIONS

This paper develops a distributed cooperative control strategy for heterogeneous DREs in hybrid AC/DC MGs within a novel energy internet paradigm. First, a comprehensive hierarchical framework and corresponding control strategy are established to achieve the following critical objectives: precise frequency/voltage restoration, fair power/current sharing and regulated bidirectional power exchange through ILCs. Moreover, theoretical stability analysis and case studies validate the controller's performance in guaranteeing transient and steady-state responses during load variations.

ACKNOWLEDGEMENT

This work was supported by National Natural Science Foundation of China(52477133), Hainan Provincial Natural Science Foundation of China (No.524RC532) and Project of Sanya Yazhou Bay Science and Technology City (No.SKJC-JYRC-2024-66).

REFERENCE

[1] J. Cao and M. Yang, “Energy internet– towards smart grid 2.0,” in 2013 Fourth International Conference on Networking and Distributed Computing, 2013, pp. 105–110.

[2] Y. Wang, T. L. Nguyen, M. H. Syed, Y. Xu, E. Guillo-Sansano, V.-H. Nguyen, G. M. Burt, Q.-T. Tran, and R. Caire, “A distributed control scheme of microgrids in energy internet paradigm and its multisite implementation,” IEEE Transactions on Industrial Informatics, vol. 17, no. 2, pp. 1141–1153, 2021.

[3] X. Huang, D. Qi, Y. Chen, Y. Yan, S. Yang, Y. Wang, and X. Wang, “Distributed self-triggered privacy-preserving secondary control of vsg based ac microgrids,” IEEE Transactions on Smart Grid, vol. 16, no. 2, pp. 850–862, 2025.

[4] T. Xu, R. Wang, H. Meng, H. Wang, Y. Ji, Y. Zhang, Q. Zheng, P. Song and J. Xiang, “A coordinated two-stage decentralized flexibility trading in distribution grids with MGs,” Protection and Control of Modern Power Systems, vol. 9, no. 5, pp. 54-69, 2024.

[5] Y. Chen, K.-W. Lao, D. Qi, H. Hui, S. Yang, Y. Yan, and Y. Zheng, “Distributed self-triggered control for frequency restoration and active power sharing in islanded microgrids,” IEEE Transactions on Industrial Informatics, vol. 19, no. 10, pp. 10635–10646, 2023.

[6] F. Guo, L. Wang, C. Wen, D. Zhang, and Q. Xu, “Distributed voltage restoration and current sharing control in islanded dc microgrid systems without continuous communication,” IEEE Transactions on Industrial Electronics, vol. 67, no. 4, pp. 3043–3053, 2020.

[7] E. Espina, R. C´ardenas-Dobson, J. W. Simpson-Porco, D. S´aez, and M. Kazerani, “A consensus-based secondary control strategy for hybrid ac/dc microgrids with experimental validation,” IEEE Transactions on Power Electronics, vol. 36, no. 5, pp. 5971–5984, 2021.

[8] H.-J. Yoo, T.-T. Nguyen, and H.-M. Kim, “Consensus-based distributed coordination control of hybrid ac/dc microgrids,” IEEE Transactions on Sustainable Energy, vol. 11, no. 2, pp. 629–639, 2020.

[9] Z. Li, Z. Cheng, J. Si, and S. Li, “Distributed event-triggered hierarchical control to improve economic operation of hybrid ac/dc microgrids,” IEEE Transactions on Power Systems, vol. 37, no. 5, pp. 3653–3668, 2022.

[10] C. Yang, T. Zheng, M. Bu, P. Li, and J. M. Guerrero, “Distributed model free adaptive control strategy for hybrid ac/dc microgrid with event triggered mechanism,” IEEE Transactions on Industrial Electronics, vol. 71, no. 8, pp. 9077–9086, 2024.

[11] A. S. Dahane and R. B. Sharma, “Hybrid ac-dc microgrid coordinated control strategies: A systematic review and future prospect,” Renewable Energy Focus, vol. 49, p. 100553, 2024.

[12] E. Jacob and H. Farzaneh, “Decentralized model predictive control of hybrid renewable microgrids for maximizing the power extraction and enhancing system operation, using a novel enumeration based-weighting factor determination method,” Results in Engineering, vol. 26, p. 105477, 2025.

[13] J. Zhang, S. Fan, C. Deng, Y. Wang, and H. Guan, “Resilient distributed secondary control for bidirectional interlinking converters in hybrid ac/dc microgrids against fdi attacks,” IEEE Transactions on Industrial Electronics, vol. 72, no. 3, pp. 3028–3038, 2025.